The Cryosphere Discuss., 6, 957–979, 2012
www.the-cryosphere-discuss.net/6/957/2012/
doi:10.5194/tcd-6-957-2012

The Cryosphere Discussions

Arctic sea ice variability and trends, 1979–2010

D. J. Cavalieri and C. L. Parkinson

Cryospheric Sciences Laboratory/Code 615, NASA Goddard Space Flight Center, Greenbelt, MD 20771, USA

Received: 14 February 2012 – Accepted: 24 February 2012 – Published: 9 March 2012

Correspondence to: D. J. Cavalieri (donald.j.cavalieri@nasa.gov)

Published by Copernicus Publications on behalf of the European Geosciences Union.

Abstract

Analyses of 32 yr (1979–2010) of Arctic sea ice extents and areas derived from satellite passive microwave radiometers are presented for the Northern Hemisphere as a whole and for nine Arctic regions. There is an overall negative yearly trend of $-51.5 \pm 4.1 \times 10^3\,\mathrm{km^2\,yr^{-1}}$ ($-4.1 \pm 0.3\,\%\,\mathrm{decade^{-1}}$) in sea ice extent for the hemisphere. The sea ice extent trends for the individual Arctic regions are all negative except for the Bering Sea: $-3.9 \pm 1.1 \times 10^3\,\mathrm{km^2\,yr^{-1}}$ ($-8.7 \pm 2.5\,\%\,\mathrm{decade^{-1}}$) for the Seas of Okhotsk and Japan, $+0.3 \pm 0.8 \times 10^3\,\mathrm{km^2\,yr^{-1}}$ ($+1.2 \pm 2.7\,\%\,\mathrm{decade^{-1}}$) for the Bering Sea, $-4.4 \pm 0.7 \times 10^3\,\mathrm{km^2\,yr^{-1}}$ ($-5.1 \pm 0.9\,\%\,\mathrm{decade^{-1}}$) for Hudson Bay, $-7.6 \pm 1.6 \times 10^3\,\mathrm{km^2\,yr^{-1}}$ ($-8.5 \pm 1.8\,\%\,\mathrm{decade^{-1}}$) for Baffin Bay/Labrador Sea, $-0.5 \pm 0.3 \times 10^3\,\mathrm{km^2\,yr^{-1}}$ ($-5.9 \pm 3.5\,\%\,\mathrm{decade^{-1}}$) for the Gulf of St. Lawrence, $-6.5 \pm 1.1 \times 10^3\,\mathrm{km^2\,yr^{-1}}$ ($-8.6 \pm 1.5\,\%\,\mathrm{decade^{-1}}$) for the Greenland Sea, $-13.5 \pm 2.3 \times 10^3\,\mathrm{km^2\,yr^{-1}}$ ($-9.2 \pm 1.6\,\%\,\mathrm{decade^{-1}}$) for the Kara and Barents Seas, $-14.6 \pm 2.3 \times 10^3\,\mathrm{km^2\,yr^{-1}}$ ($-2.1 \pm 0.3\,\%\,\mathrm{decade^{-1}}$) for the Arctic Ocean, and $-0.9 \pm 0.4 \times 10^3\,\mathrm{km^2\,yr^{-1}}$ ($-1.3 \pm 0.5\,\%\,\mathrm{decade^{-1}}$) for the Canadian Archipelago. Similarly, the yearly trends for sea ice areas are all negative except for the Bering Sea. On a seasonal basis for both sea ice extents and areas, the largest negative trend is observed for summer with the next largest negative trend being for autumn.

1 Introduction

Satellite passive microwave observations of the Earth's polar sea ice cover over the last three decades have provided the basis for studying its regional, seasonal, and interannual variabilities. The Arctic sea ice cover has exhibited a significant decline over this period (e.g., Vinnikov et al., 2006; Meier et al., 2007; Parkinson and Cavalieri, 2008; Stroeve et al., 2011a). In contrast to the Arctic, the total Antarctic sea ice cover has increased somewhat from 1979 through 2010. Analyses of the Antarctic sea ice cover for this period are presented in a companion paper (Parkinson and Cavalieri, 2012). In

TCD

6, 957–979, 2012

this study we extend the 28-yr (1979–2006) time series presented by Parkinson and Cavalieri (2008) and discuss the differences in the Arctic sea ice variabilities and trends observed between the 28-yr and 32-yr periods.

Figure 1 shows the 32-yr averaged sea ice concentration maps for March, the month of maximum sea ice extent on average, and for September, the month of minimum sea ice extent on average. Figure 1 also shows the location of each of the nine Arctic regions analyzed in this study. Much background material about Arctic sea ice and the characteristics of each of the nine regions used in the analyses is given in Parkinson et al. (1999) and in Parkinson and Cavalieri (2008) and is not repeated here. The emphasis in this study is on the changes that occurred from the previous 28-yr time series results to the current 32-yr results. In Sect. 2 we present a brief description of the data sets used and the methods employed to derive the sea ice time series. In Sect. 3 we present the results of our analyses for sea ice extents and sea ice areas. In Sect. 4, a summary of results and conclusions are presented.

2 Data sources and methods

The data set from which the sea ice extents and areas are calculated consists of sea ice concentration maps derived from the radiances obtained from the following satellite microwave radiometers: the Nimbus 7 Scanning Multichannel Microwave Radiometer (SMMR), which operated from 26 October 1978 through 20 August 1987, and the Defense Meteorological Satellite Program (DMSP) series of F8, F11, and F13 Special Sensor Microwave Imagers (SSMI), and the F17 Special Sensor Microwave Imager Sounder (SSMIS). The F8 SSMI operated from 9 July 1987 through 18 December 1991; the F11 SSMI from 3 December 1991 through 30 September 1995; and the F13 SSMI from 3 May 1995 through 31 December 2007. The F17 SSMIS provided data from 1 January 2008 through 31 December 2010.

The generation of a long-term, consistent time series of sea ice extents and areas is particularly challenging because of the use of different satellite sensors each of

TCD
6, 957–979, 2012

which may differ in their measurement wavelengths, fields-of-view, angles of incidence, ascending node times, and calibrations. In a study of the consistency of long-term observations of oceans and ice from space, Zabel and Jezek (1994) found that ocean observations must be matched at the geophysical product level rather than at the sensor radiance level, an approach that was already in use by the sea ice community. Details of the approach, including filling data gaps, reducing land-to-ocean spillover effects, reducing weather effects over ice-free ocean, and finally matching sea ice extents and areas for each pair of overlapping sensors, are discussed by Cavalieri et al. (1999).

Starting with the Nimbus 7 SMMR each subsequent sensor was matched with the previous sensor using the available period of overlap to minimize the differences. Although we did not have the desired complete year of overlap for each pair of sensors, we were able to reduce ice extent differences during periods of sensor overlap to 0.1 % or less and ice area differences to 0.6 % or less (Cavalieri et al., 1999). Most recently, we did have a complete year of overlap (2007) between the F13 SSMI and the F17 SSMIS sensors with which to match the F13 SSMI and F17 SSMIS sea ice extents and areas. A description of the methods used and the level of agreement obtained are provided by Cavalieri et al. (2012).

3 Results

Sea ice extents and areas are presented for the entire Northern Hemisphere as monthly averaged values, monthly deviations, and yearly and seasonally averaged values for the years 1979–2010. For each of the nine Arctic regions: Seas of Okhotsk and Japan, the Bering Sea, Hudson Bay, Baffin Bay/Labrador Sea, the Gulf of St. Lawrence, the Greenland Sea, the Kara and Barents Seas, the Arctic Ocean, and the Canadian Archipelago (Fig. 1) we present the monthly deviations of sea ice extents and areas. Sea ice extent and area trends by month over the 32-yr period 1979–2010 are also presented.

TCD
6, 957–979, 2012

For the purpose of providing a relative measure of the "significance" of the trends, we calculate a ratio R of the estimated trend to its standard deviation. R provides a continuous measure of "significance" and is less arbitrary than the standard 95 % or 99 % levels of statistical significance generally used. Nonetheless, these levels of significance are indicated in the trend tables to provide a reference for comparison with other published values. These levels of statistical significance are obtained using the Student's t-test with the null hypothesis of a zero trend and assuming 30 (32-2) degrees of freedom. The threshold values of R corresponding to the 95 % and 99 % levels of statistical significance are 2.04 and 2.75, respectively. Although the use of this statistical significance test has been criticized both for the use of the null hypothesis and the arbitrary levels of significance (e.g., Nicholls, 2001) and for issues related to the autocorrelation of the data (e.g., Santer et al., 2000), we still indicate these levels of statistical significance in the tables to provide a relative measure of the robustness of the trend.

3.1 Sea ice extents

Sea ice extent is defined as the cumulative area of all grid cells having at least 15 % ice concentration. The reasons for using a 15 % cutoff have been discussed previously by Parkinson and Cavalieri (2008). We first examine sea ice extent variabilities and trends for the Northern Hemisphere as a whole and then for each of the nine Arctic regions.

3.1.1 Northern Hemisphere total

A comparison of the 32-yr March and September maps of Fig. 1 with the corresponding maps for the 28-yr period (Fig. 1 in Parkinson and Cavalieri, 2008) reveals a noticeable reduction in average ice concentrations in the central Arctic for September, whereas there are fewer noticeable differences in average ice concentration for March. This seasonal difference is reflected in the summer versus winter trends for both sea ice extents and areas discussed below.

TCD
6, 957–979, 2012

Figure 2a shows the monthly average sea ice extents for the total Northern Hemisphere as well as the average seasonal cycle (Fig. 2a inset) based on monthly averages. Generally, the month of maximum extent is March, whereas the month of minimum extent is September. The three years with the largest March sea ice extents for the Northern Hemisphere were 1979, 1983, and 1982 having extents of 16.1, 15.9, and 15.8 million square kilometers, respectively. The three years with the smallest September sea ice extents were 2007, 2008, and 2010 with extents of 4.3, 4.7, and 4.9 million square kilometers, respectively.

Figure 2b shows the sea ice extent monthly deviations for the November 1978–December 2010 (32 1/6 yr) period with an overall trend of $-51.4 \pm 1.9 \times 10^3\,\mathrm{km}^2\,\mathrm{yr}^{-1}$. The largest negative excursion from the trend line occurs in September 2007, which had the smallest sea ice extent ($4.32 \times 10^6\,\mathrm{km}^2$) for the 32-yr period. The overall trend is 14 % more negative than the corresponding trend for the 28-yr period (Parkinson and Cavalieri, 2008).

Figure 2c shows both the yearly and seasonal trends for the Northern Hemisphere for the 32-yr period 1979–2010. The trend values are provided in Table 1. All the trends are negative with increasingly larger negative trends from spring, winter, autumn, and summer. A comparison of seasonal trends from the 28-yr to 32-yr period shows that for the 32-yr period the magnitude of the negative trend for summer has increased by 31 %, for autumn has increased by 20 %, for winter has increased by 1 %, but for spring, it has decreased by 4 %.

While the Northern Hemisphere yearly trend of $-51.5 \pm 4.1 \times 10^3\,\mathrm{km}^2\,\mathrm{yr}^{-1}$ for the 32-yr period (1979–2010) (Table 1) is 14 % more negative than the corresponding trend of $-45.1 \pm 4.6\,\mathrm{km}^2\,\mathrm{yr}^{-1}$ for the 28-yr period (1979–2006) reported by Parkinson and Cavalieri (2008), the changes from the 28-yr period to the 32-yr period on a regional basis were far from uniform.

3.1.2 Regional

Figure 3 shows the sea ice extent monthly deviations and their trends for each of the nine Arctic regions and for the hemisphere as a whole. Examination of the figure illustrates the very large differences in regional sea ice extent variabilities over the 32-yr period. The three regions contributing most to the overall negative trend of the Northern Hemisphere are the Arctic Ocean ($-14.4 \pm 1.5 \times 10^3$ km^2 yr^{-1}), the Kara and Barents Seas ($-13.5 \pm 0.9 \times 10^3$ km^2 yr^{-1}), and the Baffin Bay/Labrador Sea region ($-7.6 \pm 0.6 \times 10^3$ km^2 yr^{-1}) (Fig. 3). These three regions account for over half of the total area of the nine Arctic regions combined.

The yearly trends for the Arctic Ocean and Kara and Barents Seas regions (Table 1) represent increases of 45 % and 27 % in the magnitude of the negative yearly trends, respectively, compared with the corresponding yearly trends for the 28-yr period (1979–2006) reported by Parkinson and Cavalieri (2008). Other regions showing more negative trends for the longer period are the Seas of Okhotsk and Japan, the Gulf of St. Lawrence, and the Canadian Archipelago.

Some regions had less negative yearly trends for the 32-yr period compared to the 28-yr period. These included the Bering Sea, Hudson Bay, Baffin Bay/Labrador Sea, and the Greenland Sea regions (Table 1 versus Parkinson and Cavalieri, 2008). In contrast to the other eight regions, the Bering Sea had a positive trend ($+0.3 \pm 0.8 \times 10^3$ km^2 yr^{-1}) for the 32-yr period, although not statistically significant (Table 1). For the 28-yr period, the Bering Sea trend was $-0.5 \pm 1.0 \times 10^3$ km^2 yr^{-1} (Parkinson and Cavalieri, 2008).

3.1.3 Sea ice extent trends by month for all regions

Figure 4 shows the sea ice extent trends by month for the 32-yr period 1979–2010 for each of the nine Arctic regions and for the Northern Hemisphere as a whole. Most of the nine regions show either zero or negative trends for each of the 12 months. Only the Bering Sea and the Gulf of St. Lawrence show positive trends for some months. By

TCD
6, 957–979, 2012

far the largest regional negative trend occurs for the Arctic Ocean region in the month of September (Fig. 4h). The Seas of Okhotsk and Japan and the Gulf of St. Lawrence are completely free of ice during July, August, and September, whereas the Bering Sea is totally ice free only in August.

The Northern Hemisphere (Fig. 4j) shows an interesting seasonal pattern in the monthly trends. From October through May the trends become less negative, reaching a minimum trend magnitude in May, whereas from June through September the monthly trends become more negative. The Northern Hemisphere September trend almost reaches $-80 \times 10^3\,\mathrm{km}^2\,\mathrm{yr}^{-1}$. The September trends for most of the individual regions are zero or close to zero, except for the Arctic Ocean and the Canadian Archipelago regions, which have their most negative trend in September. These two regions also have zero trends for the winter months as a result of their being completely covered by sea ice of at least 15 % ice concentration in all winters of the 1979–2010 period.

A comparison of Fig. 12 in Parkinson and Cavalieri (2008) with our Fig. 4 shows that the Bering Sea had positive trends only for the months of January and February for the 1979–2006 period, in contrast to the four months of positive trends for the 32-yr period (Fig. 4b). For the Northern Hemisphere as a whole the largest negative trend occurs in September for both the 28-yr and the 32-yr periods, but for the 28-yr period the September negative trend was approximately $-57 \times 10^3\,\mathrm{km}^2\,\mathrm{yr}^{-1}$, versus the much higher magnitude $-80 \times 10^3\,\mathrm{km}^2\,\mathrm{yr}^{-1}$ trend for the 32-yr period.

3.2 Sea ice areas

Sea ice areas are defined as the cumulative sum of the product of the grid cell ice concentration and grid cell area for all grid cells having at least 15 % ice concentration. Sea ice extents are usually greater (and never less) than sea ice areas, but the two are equal for the case where all ice concentrations are 100 %. We first examine the variabilities and trends for the Northern Hemisphere as a whole and then for each of the nine Arctic regions.

TCD
6, 957–979, 2012

3.2.1 Northern Hemisphere total

Similar to Fig. 2a for sea ice extents, Fig. 5a shows the monthly average sea ice areas for the total Northern Hemisphere as well as the average seasonal cycle (Fig. 5a inset) based on monthly averages. Overall, the month of maximum sea ice area is March, closely followed by February. The month of minimum sea ice area is September. The year with the largest March sea ice area for the Northern Hemisphere is 1979, having an area of 14.2 million square kilometers, whereas the year with the smallest September sea ice area (3.1 million square kilometers) is 2007. The hemispheric yearly trend of $-49.6 \pm 4.0 \times 10^3\,km^2\,yr^{-1}$ for the 32-yr period (Table 2) is 21 % more negative than the corresponding trend of $-41.0 \pm 4.3 \times 10^3\,km^2\,yr^{-1}$ for the 28-yr period (1979–2006) reported by Parkinson and Cavalieri (2008).

Figure 5b shows sea ice area monthly deviations with an overall trend of $-49.3 \pm 1.9 \times 10^3\,km^2\,yr^{-1}$ and the year-to-year variability is almost identical to that for the sea ice extents. Likewise, the sea ice area yearly and seasonal averages shown in Fig. 5c are similar to the corresponding plots for sea ice extent, although all the values are reduced. The seasonal trends are more negative for winter, spring, autumn, and summer (Table 2 versus Parkinson and Cavalieri, 2008). We next examine the changes in trends by region. As with the sea ice extents, the changes from the 28-yr period to the 32-yr period were far from uniform.

3.2.2 Regional

Regionally and seasonally, the sea ice area variabilities are somewhat different than those for sea ice extents, reflecting the influence of sea ice concentration variability. The sea ice area trends are sometimes smaller than the corresponding sea ice extent trends, sometimes larger, and sometimes of opposite sign.

Figure 6 shows the sea ice area monthly deviations and their trends for each of the nine Arctic regions and for the hemisphere as a whole. As with the sea ice extent trends, the three regions contributing most to the overall negative sea ice area trend of

TCD
6, 957–979, 2012

the Northern Hemisphere are the Arctic Ocean ($-18.4 \pm 1.6 \times 10^3\ \text{km}^2\ \text{yr}^{-1}$), the Kara and Barents seas ($-12.3 \pm 0.8 \times 10^3\ \text{km}^2\ \text{yr}^{-1}$), and the Baffin Bay/Labrador Sea region ($-5.9 \pm 0.6 \times 10^3\ \text{km}^2\ \text{yr}^{-1}$).

When examined on a yearly average basis (Table 2), the trends for the Arctic Ocean and Kara and Barents seas regions represent increases in magnitude (more negative) of 63 % and 27 %, respectively, compared with the corresponding trends for the 28-yr period (1979–2006) reported by Parkinson and Cavalieri (2008). Other regions showing more negative trends for the longer period are the Gulf of St. Lawrence and the Canadian Archipelago.

Some regions had less negative trends for the 32-yr period compared to the 28-yr period. These included the Seas of Okhotsk and Japan, Hudson Bay, Baffin Bay/Labrador Sea, and the Greenland Sea regions. As with sea ice extent and in contrast to the other eight regions, the Bering Sea had a positive trend ($+0.5 \pm 0.6 \times 10^3\ \text{km}^2\ \text{yr}^{-1}$) for the 32-yr period. For the 28-yr period, the Bering Sea trend was negative ($-0.2 \pm 0.7 \times 10^3\ \text{km}^2\ \text{yr}^{-1}$).

3.2.3 Sea ice area trends by month for all regions

Figure 7 shows the sea ice area trends by month for each of the nine Arctic regions and for the Northern Hemisphere as a whole. While the seasonal patterns for the Northern Hemisphere and for each of the Arctic regions generally match those for the sea ice extents, there are two important differences. First, for the Northern Hemisphere, the smallest sea ice area trend occurs in March (Fig. 7j), whereas for sea ice extent the smallest trend occurred in May (Fig. 4j). As with sea ice extent, the largest negative trend occurs in September, although the magnitude of the ice area trend for October is almost as large, in contrast to the sea ice extent October value (Fig. 4j).

The second difference between the sea ice extent and area trends by month is that during the months of January through April the sea ice area trends are slightly positive for the Arctic Ocean and the Canadian Archipelago regions in contrast to the zero

TCD
6, 957–979, 2012

sea ice extent trends for the same months and regions. This implies that the sea ice concentration has been increasing over at least portions of these regions. These Arctic Ocean and the Canadian Archipelago ice area trends are somewhat less than the positive trends found by Parkinson and Cavalieri (2008) for the 28-yr period. These two regions are the only ones with statistically significant positive sea ice area trends for the winter season as a whole, although the Bering Sea has a statistically insignificant positive trend (Table 2).

For the 28-yr period (Parkinson and Cavalieri, 2008), the Bering Sea had positive trends in ice areas and ice extents only for the months of January and February, whereas for the 32-yr period, the ice areas and ice extents had positive trends from January through April (Figs. 4 and 7). Also, for the entire Northern Hemisphere, the maximum negative ice-area trends for the 28-yr period were between $50–55 \times 10^3\ \text{km}^2\ \text{yr}^{-1}$ for the months of June, July, August, and September, whereas for the 32-yr period the maximum negative ice-area trend for the month of September, is almost $-75 \times 10^3\ \text{km}^2\ \text{yr}^{-1}$.

4 Summary and conclusions

The decline of the Arctic sea ice cover continues to accelerate overall, but with significantly different regional and seasonal trends. Over the 32-yr period there was a 14 % more negative trend in yearly average sea ice extent for the entire Northern Hemisphere than for the previously analyzed 28-yr period (Parkinson and Cavalieri, 2008). Seasonally, the sea ice extent trend for the Northern Hemisphere became even more negative by 31 % for summer and by 20 % for autumn. Regionally, the largest percent change occurred for the Bering Sea which changed from a small negative trend to a small positive trend in the yearly average, but neither trend was statistically significant. Hudson Bay, Baffin Bay/Labrador Sea, and the Greenland Sea regions had somewhat smaller negative yearly average trends for the 32-yr period, whereas the Seas of Okhotsk and Japan had a slightly greater negative trend. In contrast, the Gulf of St.

TCD
6, 957–979, 2012

Lawrence, the Kara and Barents seas, the Arctic Ocean, and the Canadian Archipelago all had considerably larger negative yearly average trends than they had for the 28-yr period.

The regional, seasonal, and even monthly sea ice trend variabilities presented here reflect the complex nature of the Arctic climate system. The principal driver of the Arctic's rapidly retreating ice cover has been the long-term upward trend in Arctic air temperatures, which has been reported to be more than twice the Northern Hemisphere trend (e.g., Johannessen et al., 2004), but this Arctic amplification is not constant (Chylek et al., 2009) and may even increase in coming decades (Serreze and Barry, 2011). Superimposed on this upward trend of Arctic air temperatures has been the influence of atmospheric forcing on various spatial and temporal scales. The relationship between large-scale atmospheric circulation patterns such as the Arctic Oscillation and sea ice variability has been problematic (Stroeve et al., 2011b). Part of the problem is that even slight changes in the relative positions of low and high pressure systems and associated wind patterns will influence the growth or decay of sea ice (Maslanik et al., 2007a). Atmosphere-sea ice relationships have been found to be regionally dependent, and for a full understanding of the observed regional sea ice trends, non-linear interactions among large-scale systems need to be considered (Liu et al., 2004).

The reduction of the summer sea ice cover and its thinning have resulted in greater ocean-to-atmosphere heat transfer, reinforcing the ice-albedo feedback mechanism and leading to an accelerated loss of summer sea ice (Maslanik et al., 2007b). A complicating factor in understanding the processes driving the observed sea ice variability is that the loss of sea ice during summer has in itself had an effect on large-scale atmospheric circulation changes in the Arctic (Overland and Wang, 2010). These processes taken together with the observed rate of sea ice loss for the Arctic Ocean region during summer portends an eventual seasonal ice-free Arctic.

Acknowledgements. The authors thank Nicolo DiGirolamo and Alvaro Ivanoff for help in the preparation of the manuscript. We also acknowledge the National Snow and Ice Data Center for providing the DMSP SSMI and SSMIS daily gridded brightness temperatures used in developing the sea ice data sets. The authors gratefully acknowledge the support of NASA's Cryospheric Sciences Program for funding this work.

References

Cavalieri, D. J., Parkinson, C. L., Gloersen, P., Comiso, J. C., and Zwally, H. J.: Deriving long-term time series of sea ice cover from satellite passive-microwave multisensor data sets, J. Geophys. Res., 104, 15803–15814, 1999.

Cavalieri, D. J., Parkinson, C. L., DiGirolamo, N., and Ivanoff, A.: Intersensor calibration between F13 SSMI and F17 SSMIS for global sea ice data records, IEEE Geosci. Remote Sens. Lett., 9, 233–236, doi:10.1109/LGRS.2011.2166754, 2012.

Chylek, P., Folland, C. K., Lesins, G., Dubey, M. K., and Wang, M.: Arctic air temperature change amplification and the Atlantic Multidecadal Oscillation, Geophys. Res. Lett., 36, L14801, doi:10.1029/2009GL038777, 2009.

Johannessen, O. M., Bengtsson, L., Miles, M. W., Kuzmina, S. I., Semenov, V. A., Alekseev, G. V., Nagurnyi, A. P., Zakharov, V. F., Bobylev, L. P., Pettersson, L. H., Hasselmann, K., and Cattle, H. P.: Arctic climate change: Observed and modelled temperature and sea-ice variability, Tellus, 56*A*, 328–341, 2004.

Liu, J., Curry, J. A., and Hu, Y.: Recent Arctic sea ice variability: Connections to the Arctic Oscillation and the ENSO, Geophys. Res. Lett., 31, L09211, doi:10.1029/2004GL019858, 2004.

Maslanik, J., Drobot, S., Fowler, C., Emery, W., and Barry, R.: On the Arctic climate paradox and the continuing role of atmospheric circulation in affecting sea ice conditions, Geophys. Res. Lett., 34, L03711, doi:10.1029/2006GL028269, 2007a.

Maslanik, J. A., Fowler, C., Stroeve, J., Drobot, S., Zwally, J., Yi, D., and Emery, W.: A younger, thinner Arctic ice cover: Increased potential for rapid, extensive sea-ice loss, Geophys. Res. Lett., 34, L24501, doi:10.1029/2007GL032043, 2007b.

Meier, W. N., Stroeve, J., and Fetterer, F.: Whither Arctic sea ice? A clear signal of decline regionally, seasonally and extending beyond the satellite record, Ann. Glaciol., 46, 428–434, doi:10.3189/172756407782871170, 2007.

Nicholls, N.: Commentary and analysis: The insignificance of significance testing, B. Am. Meteorol. Soc., 82, 981–986, 2001.

Overland, J. E. and Wang, M.: Large-scale atmospheric circulation changes are associated with the recent loss of Arctic sea ice, Tellus A, 62, 1–9, doi:10.1111/j.1600-0870.2009.00421.x, 2010.

Parkinson, C. L. and Cavalieri, D. J.: Arctic sea ice variability and trends, 1979–2006, J. Geophys. Res., 113, C07003, doi:10.1029/2007JC004558, 2008.

Parkinson, C. L. and Cavalieri, D. J.: Antarctic sea ice variability and trends, 1979–2010, The Cryosphere Discuss., 6, 931–956, doi:10.5194/tcd-6-931-2012, 2012.

Parkinson, C. L., Cavalieri, D. J., Gloersen, P., Zwally, H. J., and Comiso, J. C.: Variability of the Arctic sea ice cover 1978–1996, J. Geophys. Res., 104, 20837–20856, 1999.

Santer, B. D., Wigley, T. M. L., Boyle, J. S., Gaffen, D. J., Hnilo, J. J., Nychka, D., Parker, D. E., and Taylor, K. E.: Statistical significance of trends and trend differences in layer-average atmospheric temperature time series, J. Geophys. Res., 105, 7337–7356, 2000.

Serreze, M. C. and Barry, R. G.: Processes and impacts of Arctic amplification: A research synthesis, Global Planet. Change, 77, 85–96, 2011.

Stroeve, J. C., Serreze, M. C., Holland, M. M., Kay, J. E., Maslanik, J., and Barrett, A. P.: The Arctic's rapidly shrinking sea ice cover: a research synthesis, Climatic Change, doi:10.1007/s10584-011-0101-1, 2011a.

Stroeve, J. C., Maslanik, J., Serreze, M. C., Rigor, I., Meier, W., and Fowler, C.: Sea ice response to an extreme negative phase of the Arctic Oscillation during winter 2009/2010, Geophy. Res. Lett., 38, L02502, doi:10.1029/2010GL045662, 2011b.

Vinnikov, K. Y., Cavalieri, D. J., and Parkinson, C. L.: A model assessment of satellite observed trends in polar sea ice extents, Geophys. Res. Lett., 33, L05704, doi:10.1029/2005GL025282, 2006.

Zabel, I. H. H. and Jezek, K. C.: Consistency in long-term observations of oceans and ice from space, J. Geophys. Res., 99, 10109–10120, 1994.

Table 1. Yearly and seasonal Arctic sea ice extent trends for the period 1979–2010 with estimated standard deviations*.

Region	Yearly			Winter			Spring			Summer			Autumn		
	10^3 km^2 yr^{-1}	*R*	% decade^{-1}	10^3 km^2 yr^{-1}	*R*	% decade^{-1}	10^3 km^2 yr^{-1}	*R*	% decade^{-1}	10^3 km^2 yr^{-1}	*R*	% decade^{-1}	10^3 km^2 yr^{-1}	*R*	% decade^{-1}
NH	−51.5±4.1	***12.41***	−4.1±0.3	−40.0±4.4	***9.00***	−2.6±0.3	−38.1±3.7	***10.22***	−2.8±0.3	−70.1±7.8	***8.99***	−7.9±0.9	−57.3±5.7	***10.09***	−4.9±0.5
Seas of Okhotsk and Japan	−3.9±1.1	***3.44***	−8.7±2.5	−9.2±2.9	***3.16***	−8.0±2.5	−4.9±1.8	**2.70**	−10.2±3.8	NI			−1.6±0.7	**2.15**	−9.0±4.2
Bering Sea	0.3±0.8	0.43	1.2±2.7	2.5±1.8	1.37	3.8±2.8	0.6±1.6	0.38	1.7±4.5	−0.1±0.0		−23.0±2.2	−1.5±0.9	1.71	−8.2±4.8
Hudson Bay	−4.4±0.7	***5.97***	−5.1±0.9	−0.0±0.0	1.14	−0.0±0.0	−3.1±0.7	***4.49***	−2.6±0.6	−5.7±1.2	***4.84***	−19.1±3.9	−8.6±1.6	***5.41***	−12.9±2.4
Baffin Bay/Labrador Sea	−7.6±1.6	***4.66***	−8.5±1.8	−9.5±3.2	***2.97***	−6.6±2.2	−8.0±2.0	***4.00***	−6.8±1.7	−5.1±1.1	***4.79***	−17.4±3.6	−7.9±1.5	***5.23***	−11.5±2.2
Gulf of St. Lawrence	−0.5±0.3	1.67	−5.9±3.5	−1.9±0.8	**2.22**	−8.6±3.9	−0.3±0.3	1.03	−4.3±4.2	NI			0.2±0.1	2.04	6.9±3.4
Greenland Sea	−6.5±1.1	***5.77***	−8.6±1.5	−9.5±1.9	***5.09***	−9.6±1.9	−6.0±1.2	***4.96***	−6.9±1.4	−4.8±1.6	***3.01***	−10.2±3.4	−5.7±1.4	***4.10***	−8.3±2.0
Kara and Barents Seas	−13.5±2.3	***5.80***	−9.2±1.6	−12.2±2.4	***4.98***	−6.3±1.3	−14.0±3.2	***4.44***	−7.7±1.7	−13.8±2.8	***4.86***	−18.4±3.8	−13.8±2.7	***5.08***	−10.2±2.0
Arctic Ocean	−14.6±2.3	***6.33***	−2.1±0.3	−0.2±0.1	1.34	−0.0±0.0	−2.1±0.6	***3.30***	−0.3±0.1	−38.4±6.1	***6.25***	−5.9±0.9	−17.4±2.9	***5.93***	−2.5±0.4
Canadian Archipelago	−0.9±0.4	**2.53**	−1.3±0.5	−0.0±0.0	1.10	−0.0±0.0	−0.4±0.1	**2.59**	−0.5±0.2	−2.2±1.1	**2.05**	−3.9±1.9	−1.1±0.4	***3.10***	−1.5±0.5

* Each is given as 10^3 km^2 yr^{-1} and % decade^{-1}. *R* is the ratio of the absolute value of the trend to its standard deviation. Assuming a null hypothesis of zero trend and 30 degrees of freedom, R-values in bold indicate a statistical significance of 95 %; values in italicized bold indicate a significance level of 99 %. NI means no ice.

TCD

6, 957–979, 2012

Arctic sea ice variability and trends, 1979–2010

D. J. Cavalieri and C. L. Parkinson

Title Page
Abstract | Introduction
Conclusions | References
Tables | Figures
◀| |▶
◀ ▶
Back | Close
Full Screen / Esc
Printer-friendly Version
Interactive Discussion

Table 2. Yearly and seasonal Arctic sea ice area trends for the period 1979–2010 with estimated standard deviations*.

Region	Yearly			Winter			Spring			Summer			Autumn		
	10^3 km^2 yr^{-1}	R	% decade^{-1}	10^3 km^2 yr^{-1}	R	% decade^{-1}	10^3 km^2 yr^{-1}	R	% decade^{-1}	10^3 km^2 yr^{-1}	R	% decade^{-1}	10^3 km^2 yr^{-1}	R	% decade^{-1}
NH	−49.6±4.0	***12.27***	−4.6±0.4	−31.0±4.6	***6.78***	−2.2±0.3	−42.4±4.2	***10.00***	−3.5±0.3	−69.8±6.4	***10.97***	−10.2±0.9	−54.7±6.4	***8.61***	−5.4±0.6
Seas of Okhotsk and Japan	−3.5±1.0	***3.60***	−11.9±3.3	−9.3±2.7	***3.48***	−11.4±3.3	−3.8±1.4	**2.67**	−13.1±4.9	NI			−1.1±0.5	**2.35**	−12.8±5.5
Bering Sea	0.5±0.6	0.86	2.9±3.4	2.3±1.6	1.48	5.4±3.6	0.7±1.1	0.61	3.3±5.5	−0.1±0.0		−29.1±2.5	−0.8±0.7	1.20	−8.0±6.7
Hudson Bay	−4.0±0.7	***5.47***	−5.6±1.0	−0.7±0.3	**2.46**	−0.6±0.2	−5.2±1.1	***4.62***	−5.0±1.1	−2.6±0.6	***4.12***	−19.4±4.7	−7.3±1.5	***4.78***	−14.3±3.0
Baffin Bay/Labrador Sea	−5.9±1.3	***4.42***	−8.7±2.0	−7.3±2.9	**2.57**	−6.2±2.4	−7.3±1.6	***4.72***	−8.1±1.7	−2.9±0.6	***4.96***	−19.5±3.9	−6.3±1.3	***4.75***	−12.2±2.6
Gulf of St. Lawrence	−0.5±0.2	**2.40**	−10.4±4.3	−1.7±0.6	**2.61**	−12.6±4.8	−0.3±0.1	1.77	−8.2±4.6	NI			0.1±0.0	1.21	3.3±2.8
Greenland Sea	−3.7±0.9	***4.30***	−7.2±1.7	−5.4±1.5	***3.63***	−7.7±2.1	−3.7±0.9	***4.10***	−6.2±1.5	−2.3±1.1	**2.08**	−9.2±4.4	−3.3±1.2	***2.81***	−6.8±2.4
Kara and Barents Seas	−12.2±2.1	***5.83***	−10.3±1.8	−12.6±2.7	***4.73***	−7.5±1.6	−14.9±3.0	***5.02***	−9.7±1.9	−9.2±2.1	***4.43***	−20.4±4.6	−12.3±2.6	***4.75***	−11.3±2.4
Arctic Ocean	−18.9±2.6	***7.34***	−2.9±0.4	3.0±0.8	***3.71***	0.4±0.1	−6.9±1.6	***4.29***	−1.0±0.2	−49.4±5.6	***8.87***	−9.1±1.0	−21.8±4.0	***5.42***	−3.3±0.6
Canadian Archipelago	−1.4±0.4	***3.27***	−2.3±0.7	0.7±0.1	***5.31***	1.0±0.2	−1.0±0.3	***3.11***	−1.4±0.4	−3.4±1.0	***3.34***	−8.6±2.6	−1.9±0.5	***3.50***	−2.8±0.8

* Each is given as 10^3 km^2 yr^{-1} and % decade^{-1}. R is the ratio of the absolute value of the trend to its standard deviation. Assuming a null hypothesis of zero trend and 30 degrees of freedom, R values in bold indicate a statistical significance of 95 %; values in italicized bold indicate a significance level of 99 %. NI means no ice.

TCD
6, 957–979, 2012

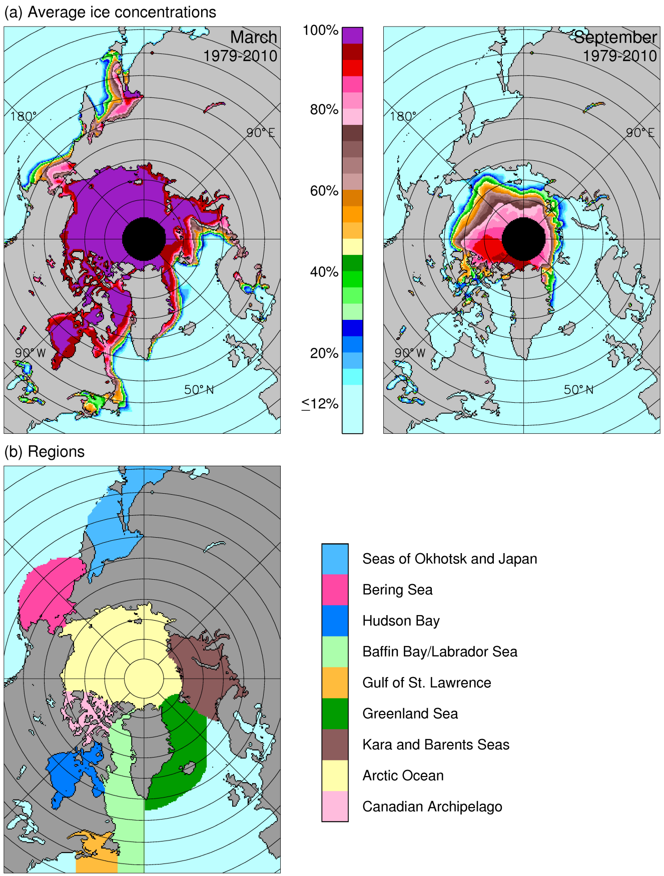

Fig. 1. (a) Maps of Northern Hemisphere March and September sea ice concentrations, averaged over the years 1979–2010, as derived from satellite passive-microwave observations. **(b)** Location map of the regions used in the analysis. (Updated Fig. 1 from Parkinson and Cavalieri, 2008).

TCD
6, 957–979, 2012

Arctic sea ice variability and trends, 1979–2010

D. J. Cavalieri and C. L. Parkinson

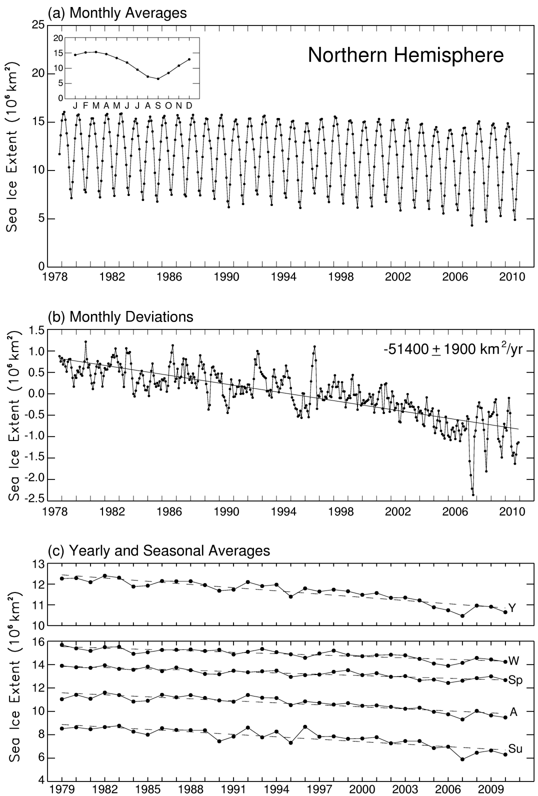

Fig. 2. (a) Monthly averaged Northern Hemisphere sea ice extents for November 1978 through December 2010. The inset shows the average annual cycle. **(b)** Monthly deviations for the sea ice extents. **(c)** Yearly and seasonally averaged sea ice extents for the years 1979–2010. The winter (W), spring (Sp), summer (Su), and autumn (A) values cover the periods January–March, April–June, July–September, and October–December, respectively.

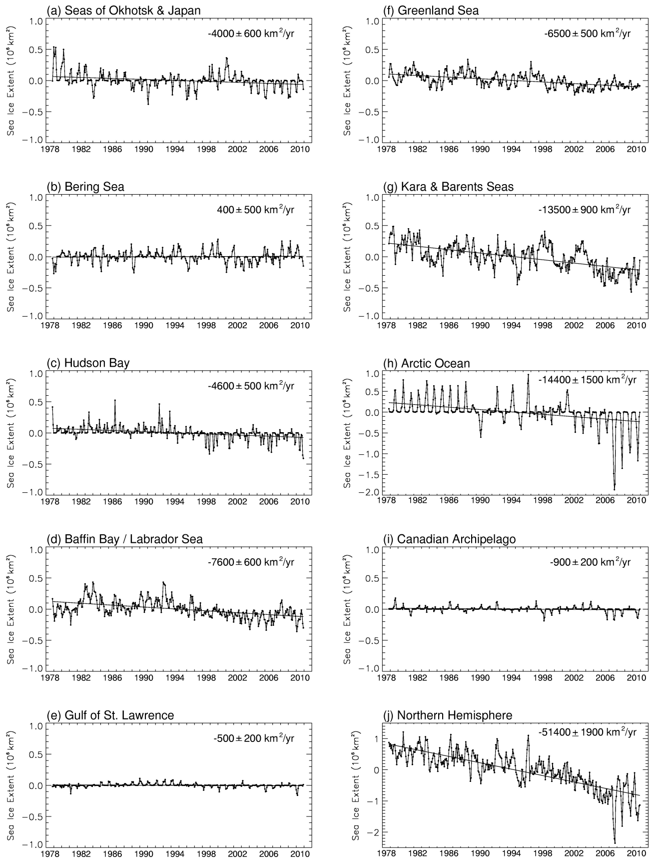

Fig. 3. Monthly deviations of the sea ice extents for: **(a)** Seas of Okhotsk and Japan, **(b)** Bering Sea, **(c)** Hudson Bay, **(d)** Baffin Bay/Labrador Sea, **(e)** Gulf of St. Lawrence, **(f)** Greenland Sea, **(g)** Kara and Barents Seas, **(h)** Arctic Ocean, **(i)** Canadian Archipelago, and **(j)** Northern Hemisphere.

TCD
6, 957–979, 2012

Arctic sea ice variability and trends, 1979–2010

D. J. Cavalieri and C. L. Parkinson

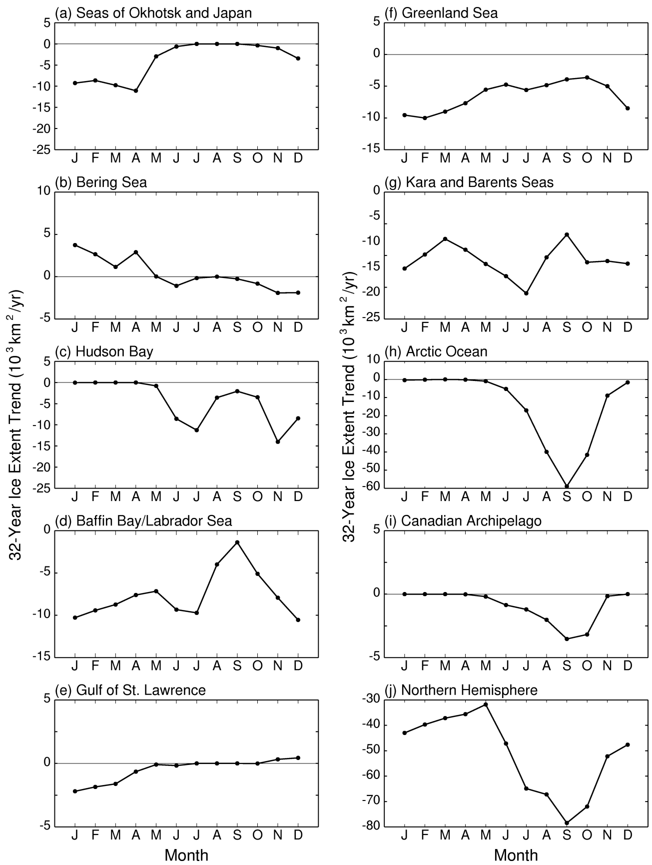

Fig. 4. Sea ice extent trends by month over the 32-yr period 1979–2010 for **(a)** Seas of Okhotsk and Japan, **(b)** Bering Sea, **(c)** Hudson Bay, **(d)** Baffin Bay/Labrador Sea, **(e)** Gulf of St. Lawrence, **(f)** Greenland Sea, **(g)** Kara and Barents Seas, **(h)** Arctic Ocean, **(i)** Canadian Archipelago, and **(j)** Northern Hemisphere.

TCD
6, 957–979, 2012

Arctic sea ice variability and trends, 1979–2010

D. J. Cavalieri and C. L. Parkinson

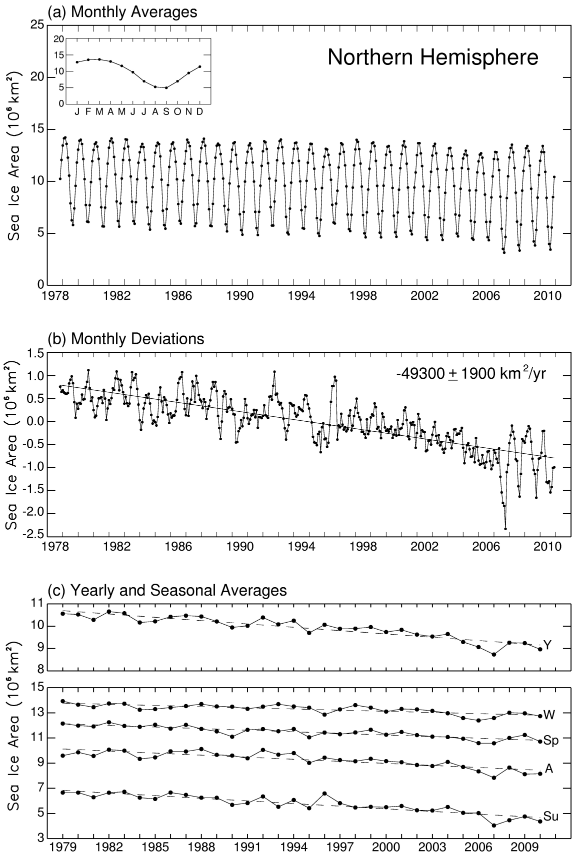

Fig. 5. (a) Monthly averaged Northern Hemisphere sea ice areas for November 1978 through December 2010. The inset shows the average annual cycle. **(b)** Monthly deviations for the sea ice areas. **(c)** Yearly and seasonally averaged sea ice areas for the years 1979–2010. The winter (W), spring (Sp), summer (Su), and autumn (A) values cover the periods January–March, April–June, July–September, and October–December, respectively.

TCD
6, 957–979, 2012

D. J. Cavalieri and C. L. Parkinson

Title Page
Abstract | Introduction
Conclusions | References
Tables | Figures
◀| |▶
◀ ▶
Back | Close
Full Screen / Esc
Printer-friendly Version
Interactive Discussion

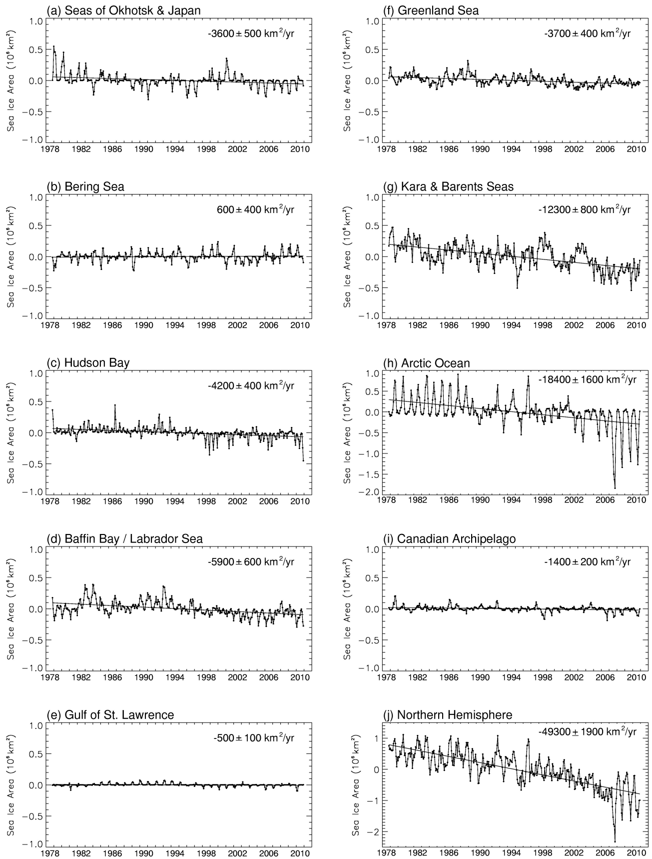

Fig. 6. Monthly deviations of the sea ice areas for: **(a)** Seas of Okhotsk and Japan, **(b)** Bering Sea, **(c)** Hudson Bay, **(d)** Baffin Bay/Labrador Sea, **(e)** Gulf of St. Lawrence, **(f)** Greenland Sea, **(g)** Kara and Barents Seas, **(h)** Arctic Ocean, **(i)** Canadian Archipelago, and **(j)** Northern Hemisphere.

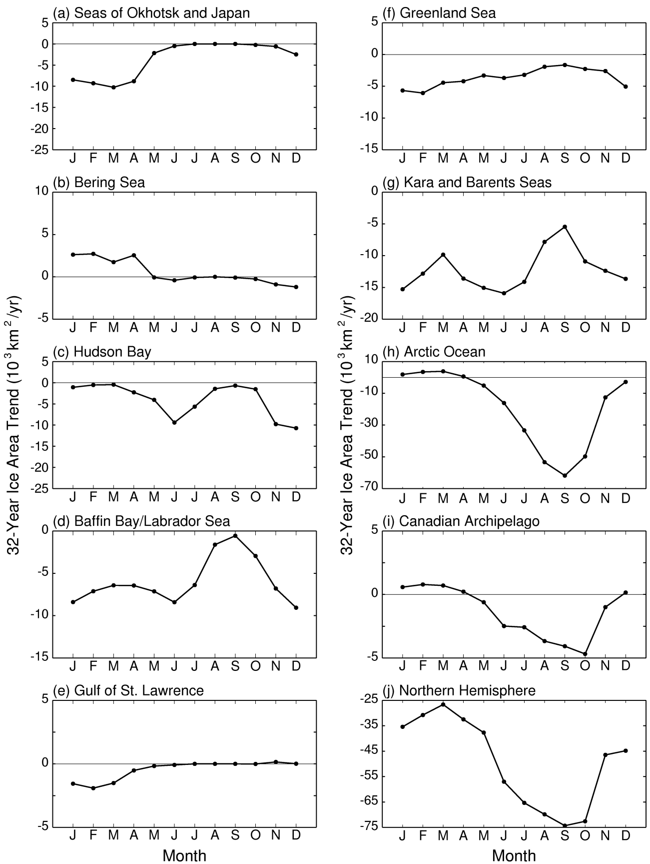

Fig. 7. Sea ice area trends by month over the 32-yr period 1979–2010 for: **(a)** Seas of Okhotsk and Japan, **(b)** Bering Sea, **(c)** Hudson Bay, **(d)** Baffin Bay/Labrador Sea, **(e)** Gulf of St. Lawrence, **(f)** Greenland Sea, **(g)** Kara and Barents Seas, **(h)** Arctic Ocean, **(i)** Canadian Archipelago, and **(j)** Northern Hemisphere.